Andreev bound states in superconductor/ferromagnet point contact Andreev reflection spectra

K. A. Yates,[1] L. A. B. Olde Olthof,[2,3] M. E. Vickers,[2] D. Prabhakaran,[4] M. Egilmez,[5] J. W. A. Robinson,[2] and L. F. Cohen[1]

[1]*Physics Department, The Blackett Laboratory, Imperial College London, SW7 2AZ, United Kingdom*

[2]*Department of Materials Science and Metallurgy, University of Cambridge, 27 Charles Babbage Road, Cambridge CB3 0FS, United Kingdom*

[3]*Faculty of Science and Technology and MESA+ Institute for Nanotechnology, University of Twente, 7500 AE Enschede, The Netherlands*

[4]*Department of Physics, Clarendon Laboratory, University of Oxford, Park Road, Oxford OX1 3PU, United Kingdom*

[5]*Department of Physics, American University of Sharjah, Sharjah 26666, United Arab Emirates*

(Received 2 June 2016; revised manuscript received 9 December 2016; published 22 March 2017)

As charge carriers traverse a single superconductor ferromagnet interface, they experience an additional spin-dependent phase angle that results in spin mixing and the formation of a bound state called the Andreev bound state. Here we explore whether point contact Andreev reflection can be used to detect the Andreev bound state and, within the limits of our experiment, we extract the resulting spin mixing angle. By examining spectra taken from $La_{1.15}Sr_{1.85}Mn_2O_7$−Pb junctions, together with a compilation of literature data on highly spin polarized systems, we suggest that the existence of the Andreev bound state would resolve a number of long standing controversies in the literature of Andreev reflection, as well as defining a route to quantify the strength of spin mixing at superconductor-ferromagnet interfaces. Intriguingly, we find that for high transparency junctions, the spin mixing angle appears to take a relatively narrow range of values across all the samples studied. The ferromagnets we have chosen to study share a common property in terms of their spin arrangement, and our observations may point to the importance of this property in determining the spin mixing angle under these circumstances.

DOI: 10.1103/PhysRevB.95.094516

I. INTRODUCTION

Point contact Andreev reflection (PCAR) spectroscopy is widely employed to determine transport spin polarization in ferromagnets (Fs). The seminal 1998 paper by Soulen *et al.* [1] opened the field, demonstrating its important application for determining the degree to which electrical currents carry an excess of one direction of spin, the so-called transport spin polarization (P). The original theoretical description of Andreev conductance across a superconductor-normal (SN) metal contact, the Blonder-Tinkham-Klapwijk (BTK) model, including a parameter Z describing the transparency of the interface [2,3], was quickly adapted to elegantly incorporate the parameter of transport spin [4]. The accessibility of the Mazin-BTK (M-BTK) method has resulted in its widespread use [5–10]. As a result of this large body of work, it is clear that certain spectroscopic features lie outside the scope of the original model, justifying the development of further descriptions of the interface properties between a superconductor (S) and a F [11–13]. In particular, other parameters have been introduced into the M-BTK fit routine, including the superconducting energy gap parameter, Δ, and a spectral broadening parameter, ω [7] (described also in terms of an effective temperature [6] or a spreading resistance [8]). Physical justification for the introduction of these parameters include the observation that Δ may deviate from the bulk value at a point contact under mechanical stress [7]. Many factors, meanwhile, can, in principle, result in spectral broadening, including a spread of interface parameters across the interface, inelastic quasiparticle scattering, inhomogeneous disorder [14,15], and, as we shall discuss below, the existence of Andreev bound states (ABS). Furthermore the effect of the Fermi velocity mismatch between the two materials making up the contact provides a contribution to Z [3,13,16], resulting in a predicted lower bound for Z (Z_{eff}) (including, in the case of Fs, a different minimum Z for each of the spin bands [13]). Fits to data resulting in $Z = 0$ are therefore unphysical, but, as we have discussed previously [16] (and summarized with literature data shown in Supplemental Material Fig. S1 [17]), the $Z = 0$ problem is a feature present in the PCAR results of many highly polarized materials [18], particularly the fully spin polarized CrO_2 [16].

The development of a theoretical framework describing SFS junctions (or π junctions) has led to a greater appreciation of the influence of the ferromagnetic exchange field on the superconducting phase difference of Josephson junctions [19–26] and the consequent contribution of ABS to the conductance [22,24,27]. Within this framework, spin mixing occurs, and each carrier experiences a spin-dependent phase as it traverses the SF boundary. This phase difference leads to the formation of a Cooper pair of the triplet form ($|\uparrow\downarrow\rangle + |\downarrow\uparrow\rangle$), and consequently ABS are expected to develop at subgap voltages in the spectra. The ABS form at voltages given by the spin mixing angle, θ [24,28]:

$$\varepsilon = \pm\Delta \cos\left(\frac{\theta}{2}\right). \tag{1}$$

In order to determine whether ABS are observed routinely in conventional S/F point contact spectra, albeit in a form that allows them to be easily overlooked, and to develop a methodology that would detect them were they to be present, we examine a series of spectra from crystals of $La_{1.15}Sr_{1.85}Mn_2O_7$ in combination with a re-examination of literature data on highly spin polarized systems [5,9,10,16]. First, we explore the temperature dependence of the zero bias conductance, which, if ABS are present in the spectra, is predicted to behave differently to the

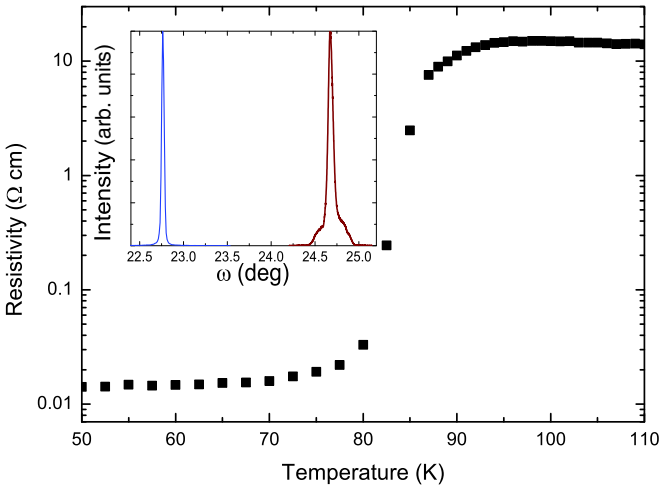

FIG. 1. Resistivity of an $La_{1.15}Sr_{1.85}Mn_2O_7$ crystal. Inset shows XRD ω scans on (0 0 10) for two samples, blue curve (left) and red curve (right).

case expected by the M-BTK. Then, individual spectra taken from $La_{1.15}Sr_{1.85}Mn_2O_7$ crystals are carefully examined to determine whether features consistent with ABS can be directly observed.

II. EXPERIMENTAL METHOD

Single crystals of $La_{1.15}Sr_{1.85}Mn_2O_7$ were grown using an optical floating zone imaging furnace method under a mixed oxygen/argon atmosphere pressurized to approximately $6–8\times10^5$ Pa. Phase identification, purity, and structural quality was determined by x-ray diffraction (XRD) and electron probe microanalysis, as described in detail elsewhere [29]. Two specimens (with an approximate volume of $2\times3\times5\,mm^3$), from the same batch as the other reported work, have been examined by high resolution XRD (HRXRD) (see the inset to Fig. 1). Omega (ω') scans gave multiple peaks, implying crystallites with slightly different orientations. Working on the strongest of these 2theta/omega ($2\theta/\omega'$) scans on four (00l) peaks mostly gave two peaks. This gives four values for the lattice parameter c: 20.068(2) and 20.076(2) Å for the first specimen and 20.078(2) and 20.083(1) Å for the second, which is a real difference in c. Comparing these numbers to previously reported data in Ref. [30] suggests a small variation (∼2% of x) in composition consistent with remarks by Prabhakaran and Boothroyd [29]. We found that lattice parameter a (which is equal to b) is almost constant at the value 3.875(3) Å. Resistivity data on an $La_{1.15}Sr_{1.85}Mn_2O_7$ crystal grown in the same batch is shown in Fig. 1. The resistivity data indicate a transition at ∼90 K, slightly lower than the ∼100 K expected for this composition [31,32], while magnetization data taken at 10 K showed a magnetic easy axis in the c direction (not shown). Point contact measurements were taken using mechanically sharpened Pb tips ($T_c = 7.2$ K) using a differential screw mechanism to slowly bring the tip into contact with the sample in a liquid helium dewar [7]. Once a contact was established, spectra were taken such that either the pressure on the contact was varied (contact resistance was changed) or the temperature of the contact was slowly increased. Where data were fitted with the M-BTK model, the $\chi^2(P)$ technique was used, whereby the spectra are fitted for Δ, Z, and ω for each value of P_{trial} [7]. The value of P is then the minimum in the $\chi^2(P_{trial})$ function, as described in Ref. [7]. The dI/dV spectra were measured directly using a standard lock-in amplifier, while the d^2I/dV^2 data were numerically derived. The IV measurements were taken simultaneously with the dI/dV measurement, for each contact.

III. RESULTS

A. States in the gap as determined by the temperature dependence of the conductance

We start with an examination of the temperature evolution of the zero bias conductance. We compare the trends with the model predictions using the M-BTK and the spin mixing model (SMM), shown in Figs. 2(a) and 2(b), respectively. Ideally, in order to distinguish between models, measurements taken at $T \ll 0.5T_c$ are required [33]. Figure 2(a) sets out the M-BTK model data, including the impact on the temperature dependent conductance of introducing additional broadening to the M-BTK model [$P = 100\%, Z = 0.1, \Delta = \Delta(T)$], plus literature data on $HgCr_2Se_4$ taken from Ref. [34], which are indeed extended to low temperatures. This latter experimental data does not fit within a M-BTK model, even with additional (temperature independent) nonthermal broadening.

Figure 2(b) shows G_0/G_n for $La_{1.15}Sr_{1.85}Mn_2O_7$ crystals (this paper) and for CrO_2 films grown onto TiO_2 (blue data) [33] and Al_2O_3 (dark yellow data) [16]. Also shown are G_0/G_n data extracted from spectra in the literature for CrO_2 grown onto TiO_2 [10]. Other literature data from highly spin polarized $La_{0.7}Sr_{0.3}MnO_3$ (LSMO3) [5] and $HgCr_2Se_4$ [34] are also compared to the SMM model predictions with varying spin mixing angles [35]. The clustering of the data in Fig. 2(b) falls in the proximity of the predicted conductance for $\theta = \pi/2$. Although it should be noted that to accurately determine θ, the spectra would need to be fitted using this model (which is outside the scope of this paper).

We note that even a moderate amount of nonthermal broadening makes the predictions of the two models harder to distinguish, particularly at $T \geqslant 0.5T_c$; therefore, more data taken to lower temperatures would be useful. However, the clustering of data close to the predictions of the SMM at $\theta = \pi/2$, coupled with the seemingly poor fit to the M-BTK, is a strong indication that ABS may be present in the spectra with a spin mixing angle close to $\theta = \pi/2$.

B. Search for ABS using d^2I/dV^2

As yet, only the study of Hübler *et al.* reports observation of ABS-like features in a number of Al-Al_2O_3-Fe tunnel junctions studied at 50 mK [36]. The data from Hübler *et al.* suggest that in the tunneling regime (low interface transmission), the absolute magnitude of the observed ABS is small (approximately three orders of magnitude smaller than the normal state conductance), requiring low temperatures for detection. The authors suggest that ABS features appeared in the conductance curves only in spatial regions where the tunneling barrier was sufficiently thin. In this regime, they found that the spin mixing angle took a broad range of values,

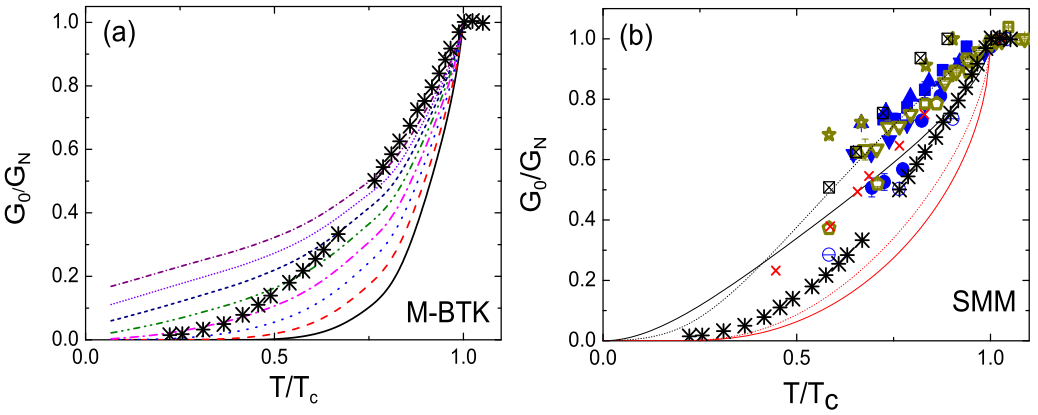

FIG. 2. (a) Temperature dependence of G_0/G_n for the M-BTK model with thermal broadening only (solid black line) and then 0.1 meV additional nonthermal broadening up to 0.7 meV additional nonthermal broadening. (*) $HgCr_2Se_4$ data taken from Ref. [34]. (b) $G_0/G_n(T)$ for the SMM, with $\theta = 0$, $Z = 0.1$ (lower curve, solid red line), 0.5 (dotted red line), $\theta = \pi/2$, $Z = 0.1$ (upper curve, solid black line), $Z = 0.5$ (dotted black line) with $La_{1.15}Sr_{1.85}Mn_2O_7$ (⊠) and extracted data for CrO_2 films onto TiO_2 (blue symbols, Ref. [33], [10]) and Al_2O_3 (dark yellow, Ref. [16]). Data extracted from literature on LSMO3 (red, x) [5] and (*) on $HgCr_2Se_4$ [34].

reflecting its sensitivity to interface properties. In contrast, the transmission probability in PCAR spectra should be considerably higher than in a tunneling measurement [28,36], allowing detection at higher measurement temperature. It is therefore reasonable to search for symmetric bumps in the point contact conductance spectra that correlate with a dip in d^2I/dV^2 in the positive voltage and a peak in the d^2I/dV^2 in the negative voltage.

A series of conductance spectra taken on $La_{1.15}Sr_{1.85}Mn_2O_7$ (LSMO) crystals were examined for evidence of ABS. The second derivative (numerically derived from the directly measured dI/dV) was scrutinised for a symmetric peak/dip signature in the $-/+$ voltage of the d^2I/dV^2. An example of a spectrum and its derivative is shown in Fig. 3(b). This composition is expected to be close to a half metal [31,37,38], and indeed fitting the spectra with the M-BTK model indicated very high values (though not 100%) for the polarization. The polarization determined from the M-BTK model is listed for four contacts in Table I, while the M-BTK fit to the data for one contact is shown in Fig. 3(a). In order to eliminate random noise from what may be a real signature of ABS, the following steps were taken:

(1) Peak/dip features in d^2I/dV^2 were identified as potential ABS if and only if they occurred symmetrically with respect to the bias voltage.

(2) Noise can occur on both the conductance and the voltage bias measurement, but genuine ABS features will appear only in the conductance. As it is measured directly, the dI/dV can be plotted either against the voltage of the contact or against the order in which the data was acquired, effectively the time. Plotting the derivative of the dI/dV (obtained numerically) vs time will therefore show features both due to noise on the conductance and features owing to genuine ABS features. Features due to noise on the voltage measurement will not be present. The derivative of the dI/dV data vs time was examined for peak/dip features symmetric about the zero bias dip in the conductance. The time associated with the zero bias can be determined by comparing the derivative plotted against time with the measured $dI/dV(t)$ [Fig. 3(c)]. Features found from the derivative of this conductance were then compared to the features that had occurred in the d^2I/dV^2 plotted against voltage. Features that appeared in both derivatives were identified as potential ABS features. In this way, features in the $d^2I/dV^2(V)$ that arise as a consequence of noise on the measurement of the voltage signal can be eliminated from further consideration.

(3) The spin mixing angles determined using Eq. (1) were compared with the spin mixing angle extracted from the IV measurements, as the IV is also expected to provide a further method for evaluating θ [35].

TABLE I. List of parameters for each contact. In the contact name, the first letter refers to the crystal studied and the second to the data set itself; therefore, V, G means the conductance data set G taken on the crystal labeled V. Z and P have been determined using the M-BTK fit procedure. The parameter ε/Δ was obtained directly from the spectra, while θ was obtained by applying Eq. (1) to ε/Δ. Two values are listed for V, H because two peaks satisfied the criteria outlined in the text. θ_{max} was determined, as described in the text.

Contact name	Resistance at 10 mV (Ω)	Z(M-BTK)	Polarization (M-BTK, %)	ε/Δ	θ from SGS	θ_{max} from IV assuming $\Delta = 1.35$ meV
III, K	66.7	0.08	81.5	0.5 ± 0.07	$(0.66 \pm 0.08)\,\pi$	$\leqslant 0.5\,\pi$
V, E	104	0	87.5	0.67 ± 0.15	$(0.5 \pm 0.2)\,\pi$	–
V, G	61.4	0.68	83 ± 3.5	0.45 ± 0.10	$(0.7 \pm 0.1)\,\pi$	$\leqslant 0.4\,\pi$
V, H	58.7	0.63	86 ± 3	0.17 ± 0.03	$(0.89 \pm 0.04)\,\pi$	$\leqslant 0.5\,\pi$
				0.74 ± 0.15	$(0.39 \pm 0.24)\,\pi$	

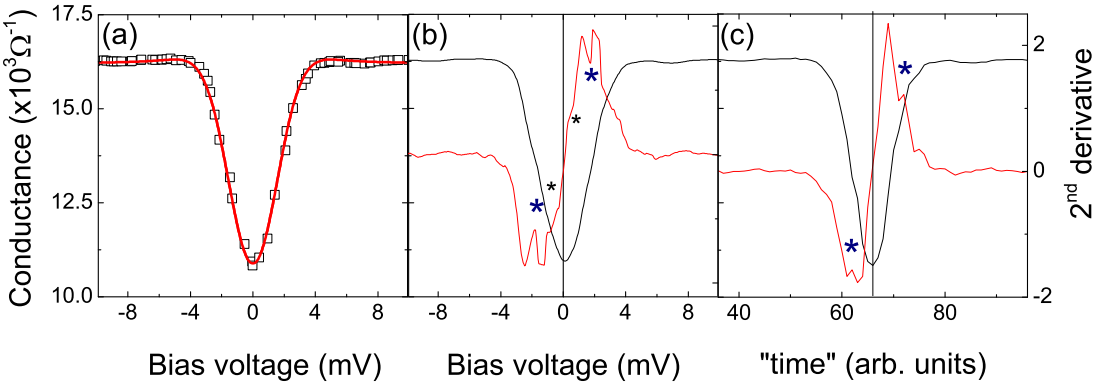

FIG. 3. (a) Conductance as a function of voltage for crystal V, contact G (squares) with the fit using the M-BTK model and $P = 83\%$, $Z = 0.68$, $\Delta = 0.9$ meV, $\omega = 1.05$ meV. (b) Conductance for the same contact with the d^2I/dV^2 showing peaks (in the negative bias) dips (in the positive bias) that may be associated with ABS. (c) Conductance for the same contact as a function of acquisition order with the derivative of that data, indicating that only the blue asterisked peak/dip feature is observed in both bias and time second derivatives.

These are strict criteria, but imposing them facilitates the extraction of only symmetric ABS, as predicted by the SMM [28].

The aim of our experiment was to obtain an examination of the evolution of the ABS (and therefore of θ) for a particular point contact when either pressure (changing the interface resistance and Z) or temperature was varied. Nineteen spectra were obtained in total on the LSMO crystals. Sixteen spectra were taken as a function of contact resistance for several contacts, while one series of three contacts was taken as a function of temperature. After analysis, 11 spectra showed features with symmetric peak/dip features in the d^2I/dV^2 vs voltage. When the contacts were further analysed with step 2, eight spectra showed near-symmetric bumps in the derivative vs row number, but only four spectra showed features in the conductance at approximately the same voltage as in the d^2I/dV^2. These four spectra are shown in Fig. 4. Of these, three spectra (contacts E, G, and H) were from a series where the contact underwent a systematic variation of pressure (changing the contact resistance on crystal V). Unfortunately, it was not possible to extract a reliable set of ABS data as a function of temperature. Using Eq. (1), the value of θ was determined from the position of these features in the d^2I/dV^2 (relative to the gap voltage estimated from the position of the conductance peak features). These values are listed in Table I. It should be noted that in the presence of broadening, the position of the coherence peaks in the measured spectra is not at the voltage value corresponding to the $T = 0$ value of Δ obtained from the M-BTK fit. To illustrate this point further, Fig. 5 shows a generated spectrum ($Z = 0.6$, $P = 90\%$, $\Delta = 0.9$ meV, $\omega =$ varying), and it can be seen how the coherence peaks spread out to higher voltages as the temperature and nonthermal broadening contribution are increased. All features occurring at voltages less than the broadened gap value (indicated by the arrow on the figure) are broadened similarly to Δ and so are subgap. Consequently, it is only possible to ascertain the ratio of ε/Δ and not an absolute value of ε. However, as it is precisely this ratio that is required in Eq. (1), this does not prevent a determination of the value of θ.

No systematic change in the extracted θ value with contact resistance was observed with contact pressure (Table I). It is, however, interesting to note that the θ values extracted from the d^2I/dV^2 method are also clustered. Athough measured in an entirely independent way, this is consistent with the clustering of data shown in Fig. 2. In combination, these observations suggest that in the junctions we have examined here, the average spin mixing angle appears to take a narrow range of values grouped around 0.5π. Our observations also suggest that the elusive ABS may indeed be evident in many low temperature Andreev point contact conductance spectra. Nonetheless, it is important to note that only a minority of spectra satisfy our rather stringent requirements. Although this consistency between different data sets is reassuring, the results are preliminary and should be treated tentatively. The robust methodology we have established to search for the ABS is of generic value.

Although the results are suggestive of ABS and it appears that we can discern their presence directly from the spectra, it is important to note that other effects could cause either ABS and/or an enhanced subgap conductance. While we have conducted as rigorous a scrutiny as our current data allows, it is important to examine whether the other mechanisms responsible for enhanced subgap conductance could play a role.

A magnetic scattering layer at some distance within the normal metal from the S-N interface produces subgap states (contributing to the conductance) caused by multiple carrier reflections between the S, the normal metal, and the magnetic scattering layer [39]. Similarly, interference effects are expected in simple SF interfaces if the F is an ultrathin layer [40,41]. Both of these cases require very specific sample geometries, and neither are valid scenarios in the samples measured here.

Joule heating in the point contact area can also produce zero bias anomalies if the contact is not in the ballistic limit (where the ballistic limit is defined as the contact diameter d, being less than the mean free path in the F [41]). However, this limit can be avoided by careful measurement and so should not be the cause of enhanced subgap conductance that has been observed systematically in CrO_2 [16,33] and (Ga,Mn)As [42], nor in the current paper.

Multiple superconducting gaps could have the effect of producing bumps in the subgap conductance [43], which may

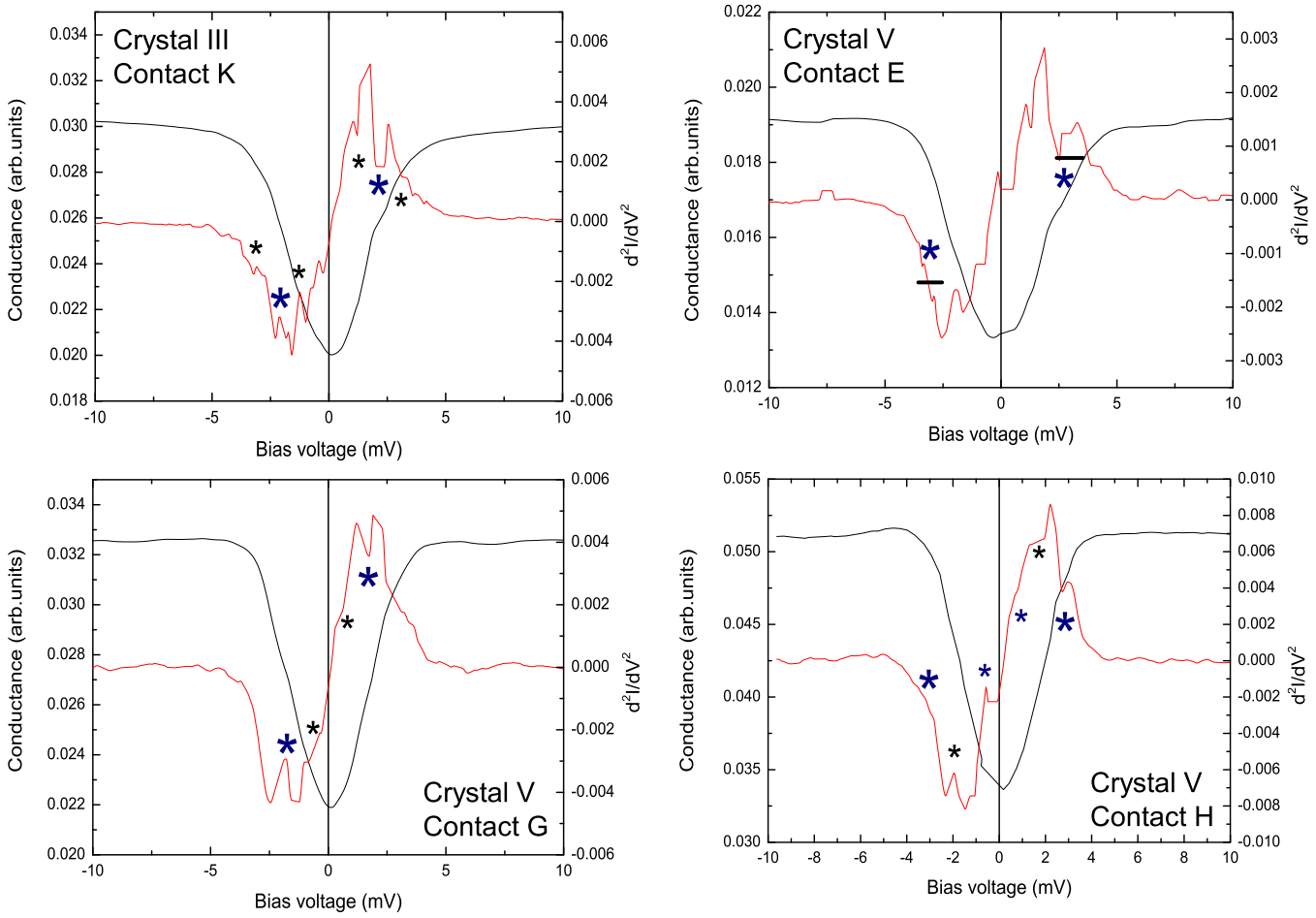

FIG. 4. Conductance and d^2I/dV^2 against bias voltage for the four contacts that satisfied criteria 1 and 2, as outlined in the text. Black asterisks show features in the d^2I/dV^2 that are symmetric in bias voltage, while the blue asterisked features appeared in both the bias voltage data and against time. For crystal V, contact H, two features in dI/dV satisfied both criteria and so are considered candidate ABS features. Bars in V, E indicate difficulty in identifying exact position of peaks/dips with criteria 1 and 2.

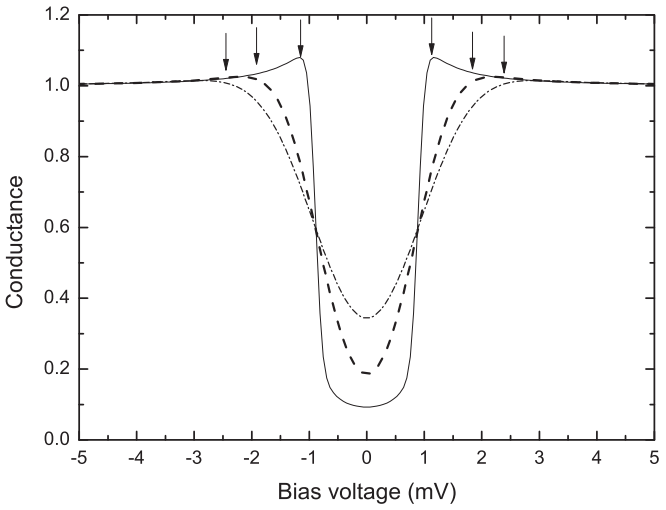

FIG. 5. Generated spectra with P=90%, Z=0.6, Δ=0.9 meV, $\omega = 0.06$ (solid line), 0.36 (dashed line), and 0.54 (dashed-dotted line) meV. The arrows show the position of the coherence peaks as they shift with broadening.

resemble the sought after ABS. However, each point contact is composed of many nanocontacts [7], so any suppression of the gap caused by inhomogeneity in the individual contacts (through mechanical stress, for example) would be expected to average over many different effective gaps. For a feature in the d^2I/dV^2 to originate from multiple gaps but to resemble a candidate ABS, as observed here, the gap distribution across the superconducting tip would have to be a bimodal distribution over a large number of contacts. In general, such a distribution is unphysical. Interestingly Ruby *et al.* [44] recently demonstrated that Pb can be considered to be a two gap S; however, the gap values are separated by 0.15 meV, which is much smaller than the separation of features that are observed in the data presented here. Therefore, we exclude this as an explanation for the observed behavior.

C. Consistency between measured θ values and IV data

Finally, in principle, the excess current can be used as a third independent check of θ [35]. The excess current is defined as IR_n/Δ. In our case, R_n was determined from the

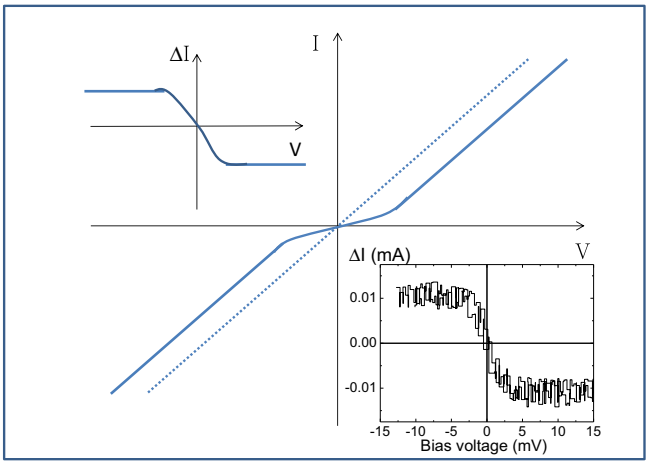

FIG. 6. Schematic of the IV graph showing current deficit (negative excess current) (solid line) against Ohmic response (dashed line). Top left inset shows an ideal data set after subtraction of the Ohmic response for determination of the excess current, while the lower right inset is data taken on crystal III, contact K.

gradient of the IV at $|5–15|$ mV, and Δ was assumed to take the bulk value (1.35 meV), as assumed in Ref. [35]. A schematic showing the excess current is shown in Fig. 6. Although the term "excess current" implies a positive value for the current in the contact compared to the Ohmic case, this is true only for Andreev contacts to nonpolarized materials. In highly polarized contacts, it is expected that there is instead a *deficit* current. Nonetheless, to ensure that the terminology remains valid for contacts to materials of varying polarization and to be consistent with Löfwander *et al.* [35], we have referred to this current deficit as a *negative* excess current. The values of this excess current were compared with Fig. 4 of Ref. [35], where the excess current is plotted as a function of Z_{SMM} for varying values of θ It is possible to place only an upper bound on θ, θ_{max} using this method because Ref. [35] assumes full spin polarization and θ_{max} is determined from reading the value off the graph (assuming $Z_{\mathrm{SMM}} = 0$). Although it would be possible to determine θ from the IV by fitting the data with the SMM, this requires the development of a new protocol for fitting with the SMM, as has been done for the M-BTK [7–9]. This is beyond the scope of the present paper, and as such the IV data can only be indicative rather than conclusive. Nonetheless, this approximation provides a consistency check. The θ_{max} values determined in this way are listed in Table I for the four contacts shown in Fig. 4. We note that the value for θ_{max} for each contact is consistently lower than θ obtained from the d^2I/dV^2, but given the limitation of the method in its present form, we find that the agreement is sufficiently convincing to support our conclusions regarding the spin mixing angle in these films.

IV. SUMMARY

In this paper, we have examined Andreev point contact spectra taken from $La_{1.15}Sr_{1.85}Mn_2O_7$ single crystal – Pb junctions and compared them with a compilation of literature Andreev point contact data on other highly spin polarized systems. Taken together, the results suggest that ABS may be present in many PCAR spectra. We develop a methodology for extracting the ABS from PCAR spectra and demonstrate that the zero bias conductance, the excess current, and the position in energy of these subgap states can be used as a set of independent checks to quantify the degree of spin mixing at the SF interface. The results and analysis suggest that the study of single SF junctions can provide a robust method to gain valuable insight into the formation of ABS and the spin mixing angle. Within the limits of the data presented, much of which have been re-examined from the literature, the average spin mixing angle appears to take a rather narrow range of values in highly spin-polarized materials, clustering around 0.5π. The Fs we have chosen to study share a common property in terms of their spin arrangement, and our observations may point to the importance of this property in determining the spin mixing angle in high transparency Andreev point contact spectra. This is in contrast to previous work examining the low transparency tunneling regime using ferromagnetic Fe, which has only partially spin polarized carriers and where it was found that the interfacial properties played a dominant role [36]. Nonetheless, the results are preliminary, and more data taken to lower temperatures would be of value. The existence of the ABS within the PCAR spectra would resolve a number of long standing puzzles, such as the $Z = 0$ problem. If ABS are present in highly spin polarized systems, fitting using the M-BTK model would result in fit parameters with high broadening and extremely low Z in order to account for the anomalously high subgap conductance caused by the presence of the ABS. An important extension of our paper would be to use the PCAR methodology in combination with external parameters that would allow direct variation of θ *in situ*. Theoretically, using microwaves to excite ferromagnetic resonance (FMR) in the ferromagnetic layer should provide exactly such an external tuning of θ [45,46]. Andreev reflection could then be used to measure a single contact repeatedly as a function of microwave excitation frequency. This would enable a systematic variation of the spin mixing angle and potentially the ability to moderate the strength of the so-called long range spin triplet proximity effect [47] in SFS junctions (which requires the formation of the ABS as a necessary component) using an external parameter. We anticipate that this will be an important development in future work.

ACKNOWLEDGMENTS

JWAR acknowledges financial support from the Royal Society, the Leverhulme Trust through an International Network Grant (No. IN-2013-033), and the EPSRC Programme Grant No. EP/N017242/1. L.F.C. and K.A.Y. acknowledge support from EPSRC Grants No. EP/J014699, No. EP/H040048, No. EP/N017242/1 and Leverhulme Trust Grant No. RPG-2016-306.

[1] R. J. Soulen Jr., J. M. Byers, M. S. Osofsky, B. Nadgorny, T. Ambrose, S. F. Cheng, P. R. Broussard, C. T. Tanaka, J. Nowak, J. S. Moodera, A. Barry, and J. M. D. Coey, Measuring the spin polarisation of a metal with a superconducting point contact, Science **282**, 85 (1998).

[2] G. E. Blonder, M. Tinkham, and T. M. Klapwijk, Transition from metallic to tunnelling regimes in superconducting microstrictions: Excess current, charge imbalance and supercurrent conversion, Phys. Rev B **25**, 4515 (1982).

[3] G. E. Blonder and M. Tinkham, Metallic to tunnelling transition in Cu-Nb point contacts, Phys. Rev. B **27**, 112 (1983).

[4] I. I. Mazin, A. A. Golubov, and B. Nadgorney, Probing spin polarisation with Andreev Reflection: A theoretical basis, J. Appl. Phys. **89**, 7576 (2001).

[5] B. Nadgorny, I. I. Mazin, M. Osofsky, R. J. Soulen Jr., P. Broussard, R. M. Stroud, D. J. Singh, V. G. Harris, A. Arsenov, and Ya Mukovskii, Origin of high transport spin polarization In $La_{0.7}Sr_{0.3}MnO_3$: Direct evidence for minority spin states, Phys. Rev. B **63**, 184433 (2001).

[6] N. Auth, G. Jakob, T. Block, and C. Felser, Spin polarization of magnetoresistive materials by point contact spectroscopy, Phys. Rev. B **68**, 024403 (2003).

[7] Y. Bugoslavsky, Y. Miyoshi, S. K. Clowes, W. R. Branford, M. Lake, I. Brown, A. D. Caplin, and L. F. Cohen, Possibilities and limitations of point contact spectroscopy for measurements of spin polarization, Phys. Rev. B **71**, 104523 (2005).

[8] G. T. Woods, R. J. Soulen Jr., I. I. Mazin, B. Nadgorny, M. S. Osofsky, J. Sanders, H. Srikanth, W. F. Egelhoff, and R. Datla, Analysis of point contact Andreev reflection spectra in spin polarization measurements, Phys. Rev. B **70**, 054416 (2004).

[9] Y. Ji, G. J. Strijkers, F. Y. Yang, C. L. Chien, J. M. Byers, A. Anguelouch, G. Xiao, and A. Gupta, Determination of Spin Polarization of Half Metal CrO_2 by Point Contact Andreev Reflection, Phys. Rev. Lett. **86**, 5585 (2001).

[10] C. S. Turel, I. J. Guilaram, P. Xiong, and J. Y. T. Wei, Andreev nanoprobe of half metal CrO_2 films using superconducting cuprate tips, Appl. Phys. Lett. **99**, 192508 (2011).

[11] K. Xia, P. J. Kelly, G. E. W. Bauer, and I. Turek, Spin-Dependent Transparency of Ferromagnet/Superconductor Interfaces, Phys. Rev. Lett. **89**, 166603 (2002).

[12] F. Taddei, S. Sanvito, and C. J. Lambert, Point contact Andreev reflection in Ferromagnet/Superconductor ballistic nanojunctions, J. Comput. Theor. Nanosci. **2**, 132 (2005).

[13] P. Chalsani, S. K. Upadhyay, O. Ozatay, and R. A. Buhrman, Andreev reflection measurements of spin polarization, Phys. Rev. B **75**, 094417 (2007).

[14] F. Magnus, K. A. Yates, S. K. Clowes, Y. Miyoshi, Y. Bugoslavsky, L. F. Cohen, A. Aziz, G. Burnell, M. G. Blamire, and P. W. Josephs-Franks, Interface properties of Pb/InAs planar structures for Andreev spectroscopy, Appl. Phys. Lett. **92**, 012501 (2008).

[15] A. Geresdi, A. Halbritter, M. Csontos, Sz. Csonka, G. Mihaly, T. Wojtowicz, X. Liu, B. Janko, and J. K. Furdyna, Nanoscale spin polarization in the dilute magnetic semiconductor (In,Mn)Sb, Phys. Rev. B **77**, 233304 (2008).

[16] K. A. Yates, W. R. Branford, F. Magnus, Y. Miyoshi, B. Morris, L. F. Cohen, P. M. Sousa, O. Conde, and A. J. Silvestre, The spin polarisation of CrO_2 revisited, Appl. Phys. Lett. **91**, 172504 (2007).

[17] See Supplemental Material at http://link.aps.org/supplemental/10.1103/PhysRevB.95.094516 for a summary of fits to data on CrO_2 with many resulting in $Z = 0$.

[18] Y. Ji, C. L. Chien, Y. Tomioka, and Y. Tokura, Measurement of spin polarization of single crystals of $La_{0.7}Sr_{0.3}MnO_3$ and $La_{0.6}Sr_{0.4}MnO_3$, Phys. Rev. B **66**, 012410 (2002).

[19] T. Yokoyama, Y. Tanaka, and A. A. Golubov, Resonant proximity effect in normal metal diffusive ferromagnet-superconductor junctions, Phys. Rev. B **73**, 094501 (2006).

[20] E. Zhao, T. Löfwander, and J. A. Sauls, Non-equilibrium superconductivity near spin-active interfaces, Phys. Rev. B **70**, 134510 (2004).

[21] M. Eschrig, Scattering problem in nonequilibrium quasiclassical theory of metals and superconductors: General boundary conditions and applications, Phys. Rev. B **80**, 134511 (2009).

[22] R. Zikić, L. Dobrosavljevic-Grujic, and Z. Radovic, Phase-dependent energy spectrum in Josephson weak links, Phys. Rev. B **59**, 14644 (1999).

[23] A. I. Buzdin, Proximity effects in superconductor-ferromagnetic heterostructures, Rev. Mod. Phys. **77**, 935 (2005).

[24] M. Fogelstrom, Josephson currents through spin-active interfaces, Phys. Rev. B **62**, 11812 (2000).

[25] A. Millis, D. Rainer, and J. A. Sauls, Quasiclassical theory of superconductivity near magnetically active interfaces, Phys. Rev. B **38**, 4504 (1988).

[26] J. C. Cuevas and M. Fogelström, Quasiclassical description of transport through superconducting contacts, Phys. Rev. B **64**, 104502 (2001).

[27] Yu. S. Barash and I. V. Bobkova, Interplay of spin-discriminating Andreev Bound States forming the 0-π transition in superconductor ferromagnet superconductor junctions, Phys. Rev. B **65**, 144502 (2002).

[28] R. Grein, T. Löfwander, G. Mataldis, and M. Eschrig, Theory of superconductor-ferromagnet point-contact spectra: The case of strong spin polarization, Phys. Rev. B **81**, 094508 (2010).

[29] D. Prabhakaran and A. T. Boothroyd, Single crystal growth of $La_{2-2x}Sr_{1+2x}Mn_2O_7$ under pressure, J. Mater. Sci.: Mater. Electron. **14**, 587 (2003).

[30] M. Kabota, H. Fujioka, K. Hirota, K. Ohoyama, Y. Moritomo, H. Yoshizawa, and Y. Endoh, Relation between crystal and magnetic structures of layered manganite $La_{2-2x}Sr_{1+2x}Mn_2O_7$, J. Phys. Soc. Jpn. **69**, 1606 (2000).

[31] J. Dho, W. S. Kim, H. S. Vhoi, E. O. Chi, and N. H. Hur, Re-entrant charge ordering behaviour in the layered manganites $La_{2-2x}Sr_{2x}Mn_2O_7$, J. Phys.: Condens. Matter. **13**, 3655 (2001).

[32] E. Dagotto, T. Hotta, and A. Moreo, Colossal magnetoresistant materials: the key role of phase separation, Phys. Rep. **344**, 1 (2001).

[33] K. A. Yates, M. S. Anwar, J. Aarts, O. Conde, M. Eschrig, T. Löfwander, and L. F. Cohen, Andreev spectroscopy of CrO_2 thin films on TiO_2 and Al_2O_3, Europhys. Lett. **103**, 67005 (2013).

[34] T. Guan, C. Lin, C. Yang, Y. Shi, C. Ren, Y. Li, H. Weng, X. Dai, Z. Fang, S. Yan, and P. Xiong, Evidence for Half-Metallicity in n-type $HgCr_2Se_4$, Phys. Rev. Lett. **115**, 087002 (2015).

[35] T. Löfwander, R. Grein, and M. Eschrig, Is CrO_2 Fully Spin Polarized? Analysis of Andreev Spectra and Excess Current, Phys. Rev. Lett. **105**, 207001 (2010).

[36] F. Hübler, M. J. Wolf, T. Scherer, D. Wang, D. Bechmann, and H. v. Löhneysen, Observation of Andreev Bound States

at Spin-Active Interfaces, Phys. Rev. Lett. **109**, 087004 (2012).

[37] J. W. Freeland, K. E. Gray, L. Ozyuzer, P. Berghuis, E. Badica, J. Kavich, H. Zheng, and J. F. Mitchell, Full bulk spin polarization and intrinsic tunnel barriers at the surface of layered manganites, Nat. Mater. **4**, 62 (2005).

[38] Z. Sun, Q. Wang, J. F. Douglas, H. Lin, S. Sahrakorpi, B. Barbiellini, R. S. Markiewicz, A. Bansil, A. V. Fedorov, E. Rotenberg, H. Zheng, J. F. Mitchell, and D. S. Dessau, Minority-spin t_{2g} states and the degree of spin polarization in ferromagnetic metallic $La_{2-2x}Sr_{1+2x}Mn_2O_7$ ($x = 0.38$), Sci. Rep. **3**, 3167 (2013).

[39] J-X. Zhu and Z. D. Wang, Magnetic scattering effects on quantum transport in normal metal-superconductor junctions, Phys. Rev. B **55**, 8437 (1997).

[40] J. Koltai, J. Cserti, and C. J. Lambert, Andreev Bound States for a superconducting ferromagnetic box, Phys. Rev. B **69**, 092506 (2004).

[41] G. Deutscher, Andreev-Saint-James reflections: A probe of cuprate superconductors, Rev. Mod. Phys. **77**, 109 (2005).

[42] S. Piano, R. Grein, C. J. Mellor, K. Vybarny, R. Campion, M. Wang, M. Eschrig, and B. L. Gallagher, Spin polarization of (Ga,Mn)As measured by Andreev spectroscopy: The role of spin active scattering, Phys. Rev. B **83**, 081305 (2011).

[43] D. Daghero, M. Tortello, P. Pecchio, V. A. Stepanov, and R. S. Gonnelli, Point contact Andreev-reflection in anisotropic superconductors: The importance of directionality, Low Temp. Phys. **39**, 199 (2013).

[44] M. Ruby, B. W. Heinrich, J. I. Pascual, and K. J. Franke, Experimental Demonstration of a Two-Band Superconducting State for Lead Using Scanning Tunneling Spectroscopy, Phys. Rev. Lett. **114**, 157001, (2015).

[45] S. Takahashi, S. Hikino, M. Mori, J. Martinek, and S. Maekawa, Supercurrent Pumping in Josephson Junctions With a Half-Metallic Ferromagnet, Phys. Rev. Lett. **99**, 057003 (2007).

[46] S. Hikino, M. Mori, S. Takahashi, and S. Maekawa, Microwave-induced supercurrent in a ferromagnetic Josephson junction, Supercond. Sci. Technol. **24**, 024008 (2011).

[47] J. Linder and J. W. A. Robinson, Superconducting spintronics, Nat. Phys. **11**, 307, (2015).